Journal of Hydrosciences and Environment
ISSN: 2345-5608

Calculation of local boundary shear stress in trapezoidal sections using velocity data

B. Malvandi[1] and M. F. Maghrebi[2*]

1, Ph.D. candidate of Civil Engineering Department, Ferdowsi University of Mashhad
2,- Professor of Civil Engineering Department, Ferdowsi University of Mashhad*

ARTICLEINFO

Article history:

Received: 27 March 2023
Accepted: 3 May 2023

Keywords:

Open channel

Boundary shear stress

Trapezoidal cross-section

ABSTRACT

The velocity of only one point from normal to the wetted perimeter must be known to obtain local shear stress at a point along the wetted perimeter. Then, the local shear stress on the wetted perimeter is calculated using the viscous shear stress relation and defining the non-dimensional variable ξ. ξ is considered a parametric function of some non-dimensional hydraulic and geometric variables of channel and fluid. Several experimental data are used to achieve a general form for the function, and the parameters are obtained by minimizing the MAPE (Mean Absolute Percentage Error). MAPE between the data observed and calculated by a genetic algorithm is minimized to modify the model for trapezoidal sections. Experimental data from twenty trapezoidal sections have been selected. Twelve are used for training, and the remaining eight are for testing. The average value of MAPE is 7.1%. However, one section is rectangular, with a calculated MAPE of about 16%. The high discontinuity of the wetted perimeter of the rectangular cross-section due to the 90 ° angle between the bed and the walls is responsible for approximately a large amount of MAPE. MAPE is less than 7% in 14 selected sections.

1. Introduction

Awareness of the shear stress distribution along the wetted perimeter of open channels is crucial in hydraulic engineering problems, including bank erosion, sedimentation, deposition, and stable channel design (Dey and Lambert, 2005). The most influential parameters in the shear stress distribution are channel geometry, secondary flows, and boundary roughness distribution (Knight et al., 1984). Shear stress distribution can be measured directly or indirectly. Lippmann and Davan (1952) directly measured the wetted perimeter in the air by measuring shear force on a small floating element isolated from the surface. Another technique for directly measuring the boundary shear stress distribution was used by Ghosh and Roy (1970). They separated a certain length from a long channel and suspended it according to the side and bottom gaps. Park et al. (2015) directly measured low-shear stress under high-velocity flow conditions. A tool to directly measure low shear stress was developed and validated. Direct measurement of bed shear stress using a plate or shear cell is complex, requires precise calibration, and is only suitable for some laboratory studies (Graham et al., 1992; Rankin and Hirs, 2000). These procedures are not applicable in rivers. Consequently, boundary shear stresses are preferred for indirect determination (Wilcock, 1996). Indirect methods of measuring boundary shear stress are almost based on measuring velocity or defining the relationship between velocity and distance from the boundary (Preston, 1954;

*Corresponding author's email: maghrebi@um.ac.ir

Cheng, 2007). A standard indirect method used in the study of the boundary layer includes measuring the velocity and characteristics of the normal

pressure up to the limit in successive sections and solving the cut (Ghosh and Roy, 1970). Preston (1954) developed a simple technique for estimating local shear at smooth boundaries using a pitot tube in contact with the surface, considering an internal velocity law. Another indirect method based on the logarithmic velocity distribution proposed by Prandtl-Karman involves estimating the velocity profile along normal lines to the boundary. In the indirect methods mentioned, to estimate the local shear stress of a point at the boundary, the velocity must be measured at some points in a normal line to the boundary that may be very close. The experimental works presented empirical equations for shear force distribution in different boundary parts for trapezoidal and compound channels (Rhodes and Knight, 1994; Khatua and Patra, 2007). Knight (1981) presented empirical equations for the boundary shear on the wall and the bed of rectangular cross-sections. Knight et al. (1984) derived empirical equations for the percentage of the total shear force on the sidewalls as a function of aspect ratio b/h. Flintham and Carling (1988) provided mean bed and sidewall shear stress equations in straight symmetric rectangular and trapezoidal rough cross sections. Knight et al. (1994) presented equations to estimate the mean and maximum boundary shear stresses on the bed and sidewalls. Malvandi and Maghrebi (2021) presented a model for estimating the shear stress distribution along the wetted perimeter using cross-sectional velocity data. By defining the non-dimensional variable ξ and replacing the velocity slope with the velocity to distance, they used the viscous shear stress relationship to evaluate the local shear stress at the boundary. They considered ξ as a parametric function of non-dimensional variables of cross-section, channel, and fluid properties. They calculated their relation parameters by applying their model to experimental data of seven cross-sections investigated by some researchers and minimizing the MAPE as the objective function. According to their proposed model, knowing the velocity of just one cross-section point is crucial to obtain shear stress on a selected point of the wetted perimeter. Some specifications of the fluid and channel are also necessary to introduce a new parameter that imports the viscous shear stress relation. This paper has selected the results of twenty trapezoidal cross-sections to minimize MAPE and calibrate the relationship to verify their model for trapezoidal channels only. The Genetic Algorithm is selected to minimize the objective function.

2. Materials and Methods

A model was proposed to estimate the shear stress distribution along the wet perimeter (Malvandi and Maghrebi, 2021). In the proposed model, the boundary-layer flow on a wide flat plate, as shown in Fig. 1, is considered with the governing Eq. (1):

$$\tau = \mu \frac{\partial \bar{u}}{\partial y} - \rho \overline{u'v'} = \tau_{lam} + \tau_{turb} \quad (1)$$

In the above equation, μ and ρ are the dynamic viscosity and density of the fluid, respectively, u is the component of the velocity vector in the main flow direction, and v is the vertical velocity component along the y direction (see Fig. 1), "′" denotes fluctuations and "¯" is the time mean, τ, τ_{lam} and τ_{turb} are the total, viscous and turbulent shear stresses, respectively. The term $-\rho\overline{u'v'}$ which is defined as the turbulent shear stress along y coordinate normal to the wall has a near-zero value on the boundary (see Fig. 1 (a)), and the total shear stress on the boundary is equal to the viscous shear stress as follow:

$$\tau = \mu \left(\frac{du}{dy} \right)_w \quad (2)$$

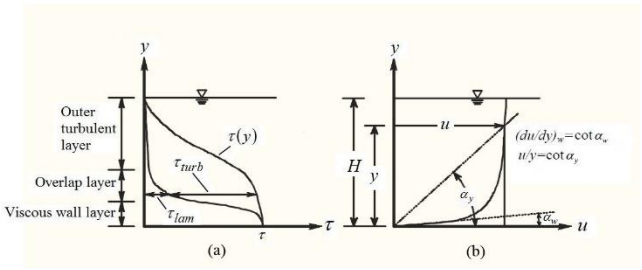

Fig.1. Typical velocity and shear stress distributions in developed turbulent flow near a wall: (a) shear stress and (b) velocity profile (Malvandi and Maghrebi, 2021).

Using this relation needs velocity measurement at some points very close to the boundary to achieve the velocity gradient at the wall (du/dy)w. Because of the difficulties of doing that, introducing ξ as the ratio of velocity to distance at a distant point from the wall (u/y) to velocity gradient at the wall (du/dy)w, the above equation is replaced by Eq. (3). Only by obtaining ξ the formidable task of calculating (du/dy)w is replaced by the easy measuring the velocity u at a considerable distance of y from the wall. So, Eq. (3) gives the possibility of measuring the velocity of flow u at a far distance, y, from the wall to calculate the viscous shear stress at the wall, which is equal to the total shear stress:

$$\tau = \mu\xi \frac{u}{y} = \mu\xi \cot \alpha_y \quad (3)$$

For a fully developed flow in an open channel, flow through the cross-section is considered near different walls, and the mentioned procedure can evaluate the shear stress at any point of the boundary. The normal distance from each wall differs, so it is shown by d instead of y.

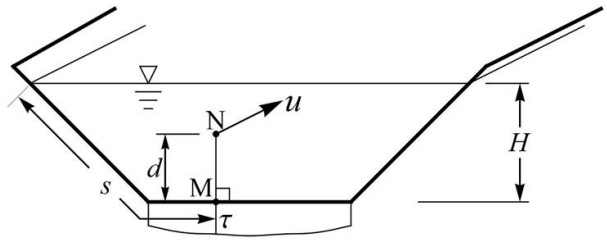

Fig.2. The schematic cross-section with the model parameters

To obtain the shear stress of an arbitrary point on the boundary, such as M in Fig. 2, the velocity of a point at its normal distance d from it, such as point N, must be known. By defining a non-dimensional variable ξ and substituting the velocity to distance ratio (u / d) for the velocity gradient (du / dy), the shear stress at point M is calculated as Eq. (4) using the viscous shear stress relation:

$$\tau = \mu \xi \frac{u}{d} \quad (4)$$

where τ is the shear stress at point M at the boundary, and u is the flow velocity at point N at a normal distance d from the boundary shown in Fig. (2). Eq. (4) is valid for the flow on a wide flat plate without restraining walls and free to extend. However, the proposed method uses this equation for the flow in a cross-section with different walls. So, flow at an arbitrary point of the cross-section affects several walls, and inversely, the shear stress at a selected point of a wall is affected by other wall effects. The effects of the other cross-section walls are considered here by interfering with the cross-sectional parameters: the area of the flow section A, the wetted perimeter P, the length of the free surface of water T, the water depth H and the distance along the wetted perimeter (starting at the left bank on the free surface, looking downstream) s. Additionally, the mean value of boundary shear stress, which can be obtained by integrating the local shear stress along the wetted perimeter, is calculated by the below equation:

$$\tau_0 = \gamma R s_f \quad (5)$$

Therefore, the local shear stress must be dependent on the fluid density ρ and the slope of the energy line sf, and considering the below function defines Eq. (4), local shear stress:

$$\tau = f\,(\mu, u, s_f, A, T, P, \rho, H, s, d) \quad (6)$$

Using dimensional analysis, ξ is defined as:

$$\xi = \frac{\tau}{\mu}\frac{d}{u} = \varphi\left(s_f, \frac{A}{TH}, \frac{T}{H}, \frac{P}{H}, \frac{d}{P}, \frac{s}{P}, \mathrm{Re}\right) \quad (7)$$

Finally, by selecting the products of the non-dimensional parameter exponents, ξ is a function of some non-dimensional cross-section, channel, and fluid properties shown in Eq. (8):

$$\xi = a_0 (s_f)^{a_1} \left(\frac{A}{TH}\right)^{a_2} \left(\frac{T}{H}\right)^{a_3} \left(\frac{P}{H}\right)^{a_4} \left(\frac{d}{P}\right)^{a_5} \left(\frac{s}{P}\left(1-\frac{s}{P}\right)\right)^{a_6} (\mathrm{Re})^{a_7} \quad (8)$$

where Re is the Reynolds number.

For each pair of points (M, N) M on the boundary and N at the cross-section, which is selected in a normal line to the boundary at the point M, there is a unique ξ that can be calculated by Eq. (4). Therefore, by moving along the wetted perimeter or a unique normal, ξ differs from one pair of points to another. To achieve a global relationship to calculate the shear stress distribution along the wetted perimeter of the trapezoidal section, some experimental data containing shear stress and velocity at several pairs of points (M, N) are necessary. Using Eq. (4) for the data, the measured values of ξm are obtained. The values calculated by the proposed model ξc are obtained using Eq. (8). An error function is then selected between the measured and calculated values, such as MAPE, as the objective function defined in Eq. (9). The parameters a0 to a7 in Eq. (8) are calculated by minimizing the objective function. In this study, a genetic algorithm is used to minimize the objective function:

$$MAPE\,(\%) = \frac{1}{n}\sum \frac{(\xi_c - \xi_m)}{\xi_m} \times 100 \quad (9)$$

where n is the number of data cases.

For an arbitrary trapezoidal channel, knowing the parameters a0 to a7, after evaluating the required cross-sectional characteristics of the channel and fluid, we can use Eqs. (8) and (4) calculate ξ and shear stress τ at any point on the wetted perimeter, respectively. As seen in Eq. (8), non-dimensional independent parameters of the relation which must be obtained are constant for a unique cross-section of a channel. They are calculated once, except for d/P and s/P, which must be calculated separately for each pair of points (M, N). Two sets of experiments performed by a number of researchers on trapezoidal open channels have been considered to evaluate the model in this paper. The first set is related to SERC flood facilities. The model can be validated using channels where the velocity distribution (perhaps in isolated lines) is known. The shear stress distribution along the wetted perimeter of the cross-section is given. The cross-sectional characteristics can be seen in Table 1. Some of the parameters listed are shown in Fig. 3. Table 1 shows the cross-sectional characteristics of the twenty trapezoidal cross-sections used to calibrate the proposed model. As observed, the last case is a rectangular cross-section that can be considered a unique trapezoid with lateral angles of 90 degrees. 60% of cases (12 cross-sections) were selected for training, and the remaining 40% (8 cross-sections) were selected for testing to validate the model. The average MAPE value for each item is calculated according to the different numbers of data observed in the channels. The average MAPE value for all selected items is considered the objective function.

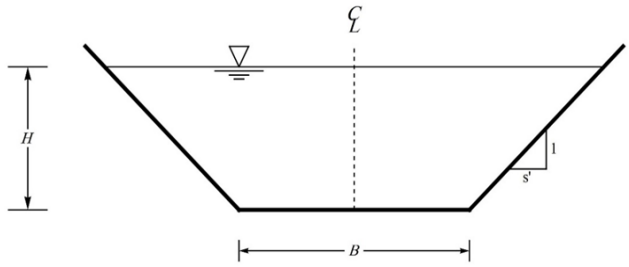

Fig.3. The schematic cross-section with some hydraulic parameters

Table 1. The cross-section and flow properties

Cross-section			B (m)	H (m)	s'	T (m)	A (m^2)	P (m)	s_f (10^{-3})	Re
(*a*)	IB0501_3	Knight and Sellin (1987)	1.5	0.049	1	1.597	0.075	1.638	1.024	63168
(*b*)	IB1001_1		1.5	0.101	1	1.702	0.162	1.785	1.017	200556
(*c*)	IB1002_4		1.5	0.101	1	1.702	0.162	1.785	1.017	200556
(*d*)	IB1501_1		1.5	0.150	1	1.8	0.248	1.925	1.035	368262
(*e*)	IB1502_3		1.5	0.149	1	1.798	0.245	1.921	1.008	369236
(*f*)	IB7501_1		1.5	0.076	1	1.651	0.119	1.714	1.021	129206
(*g*)	040101_6	Knight and Shiono (1990)	1.5	0.158	1	1.816	0.262	1.947	1.019	402791
(*h*)	040201_4		1.5	0.166	1	1.832	0.277	1.97	1.032	429569
(*i*)	040301_3		1.5	0.175	1	1.851	0.294	1.996	1.027	466804
(*j*)	040401_3		1.5	0.187	1	1.874	0.315	2.029	1.022	512038

(*k*)	040501_6		1.5	0.199	1	1.898	0.339	2.064	1.028	562091
(*l*)	040601_3		1.5	0.213	1	1.927	0.366	2.104	1.034	613059
(*m*)	040701_3		1.5	0.247	1	1.995	0.432	2.2	1.052	768592
(*n*)	040701_4		1.5	0.247	1	1.995	0.432	2.2	1.052	768592
(*o*)	040801_3		1.5	0.296	1	2.092	0.531	2.337	1.053	972352
(*p*)	040802_3		1.5	.301	1	2.102	0.542	2.351	1.039	991511
(*q*)	T03	Tominaga *et al.* (1989)	0.2	.091	1.04	0.389	0.027	0.461	0.594	87600
(*r*)	T13		0.248	0.11	0.577	0.398	0.036	0.514	0.389	64800
(*s*)	T23		0.152	0.071	1.6	0.398	0.02	0.436	0.594	53400
(*t*)	S12		0.4	0.102	0	0.4	0.041	0.603	0.138	50700

3. Result and discussion

The values obtained from the parameters of Eq. (8) and MAPE for all data are shown in Table 2. It can be seen from Table 2 and Eq. (8) that P / H is the most influential factor in ξ, and after that, d/P and Re are two parameters that have the main rules in ξ. In addition, ξ is inversely related to sf. In other words, if sf is magnified and other factors remain constant, ξ acquires a smaller value. In comparison with the earlier presented relation for different cross-sections (Malvandi and Maghrebi, 2021), it can be seen that the factor a0 magnified more than three times. Still, the exponents a1 to a7 varied up to 64 percent.

Table 2. The calculated values of the parameters and *MAPE*

a_0	a_1	a_2	a_3	a_4
0.005	-	-	-	1.258
	0.074	0.505	0.378	
a_5	a_6	a_7	*MAPE* (%)	
0.897	0.167	0.808	7.1	

The statistical parameter MAPE takes different values for different sections, with an average value of 7.1%. Figure 4 shows the values of ξ calculated by the model proposed in Equation (8) versus the values of ξ using the experimental data obtained from Equation (4) for all sections normalized by ξmax. In each section, ξmax is the maximum value of ξ among measured and calculated values. The 10% error range is also shown in Figure 4. This figure shows that the proposed model provides good results in most cases. Two cases, 040601_3 and S12, have a maximum number of points with an error of more than 10%. S12 is the only rectangular cross-section, and many of its data points predict a large amount of MAPE. Figure 4 shows that in the cases with a higher amount of MAPE, by increasing the value ξ more differences between the measured and calculated values are seen (cases 040601_3, 040801_3, 040802_3, and S12). Using Eq. (8) to calculate ξ, considering constant values for the other variables in a channel, the only influential factors in ξ are d/P and s/P. In the mentioned cases, the error increases by increasing the distance of the selected point to record velocity from the boundary, especially for closer parts of the wetted perimeter to the centerline where s/p achieves 0.5. Therefore, to avoid high error values, selecting nearer points to the boundary for recording velocity is better. Table 3 shows the MAPE values for all sections. As shown in Table 3, the MAPE is less than 10% at seventeen cross-sections, and in two cases, one of which is rectangular (S12), it reaches a maximum value of nearly 16%. The effects of severe discontinuity of the wetted perimeter in the corners are responsible for this.

Table 3. The values of *MAPE* obtained for the cross-sections

Cross-sectio	IB0501_3	IB1001_1	IB1002_4	IB1501_1	IB1502_3	IB7501_1	040101_6	040201_4		040301_3	
MAPE (%)	5.98	5.85	5.89	4.89	4.99	5.12	6.48	4.03		4.96	
Cross-sectio	040401_3	040501_6	040601_3	040701_3	040701_4	040801_3	040802_3	T03	T13	T23	S12
MAPE (%)	4.80	5.18	16.62	9.72	10.25	8.52	6.95	4.07	7.04	5.25	15.5

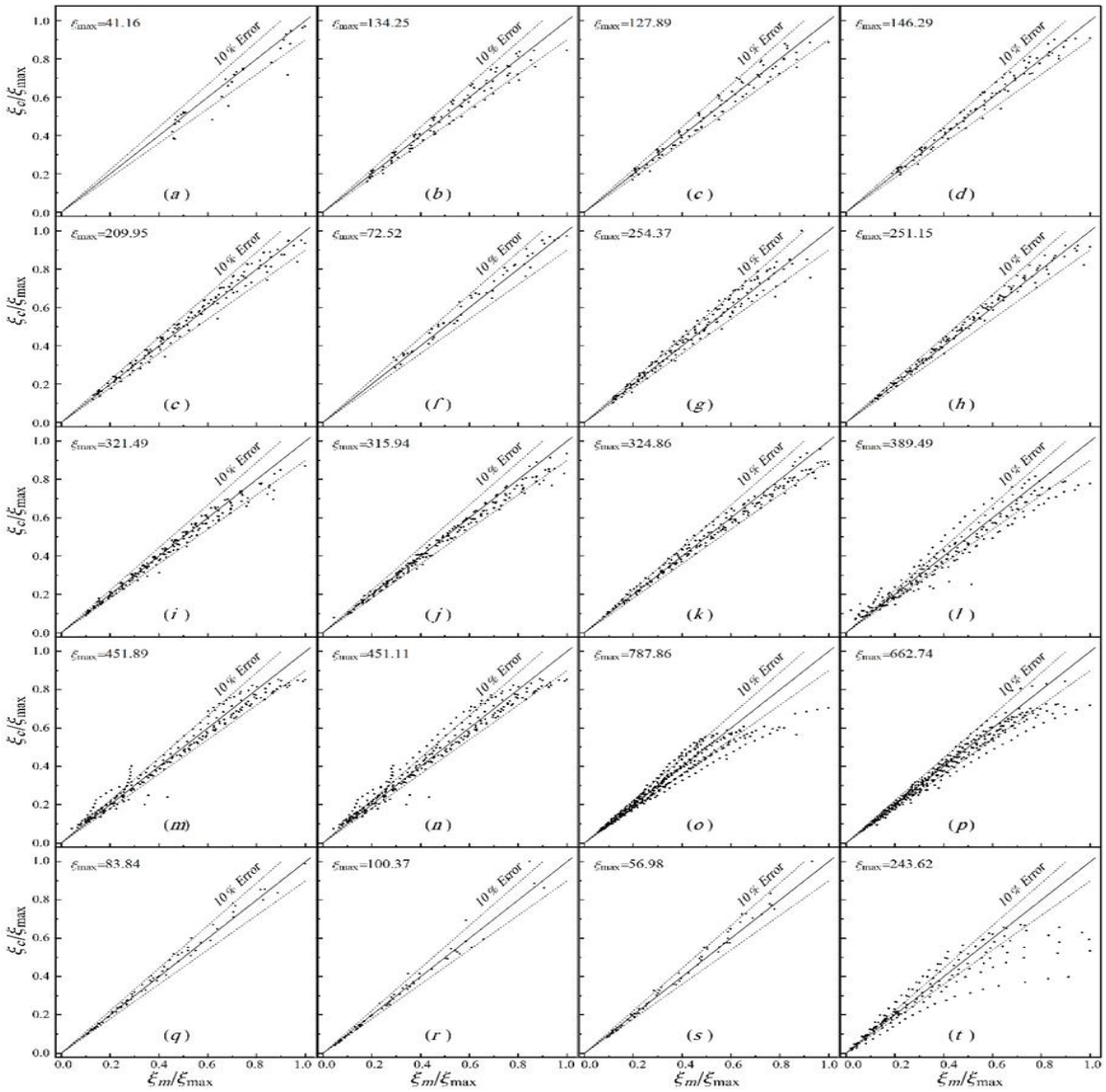

Fig.4. Normalized measured and calculated ξ

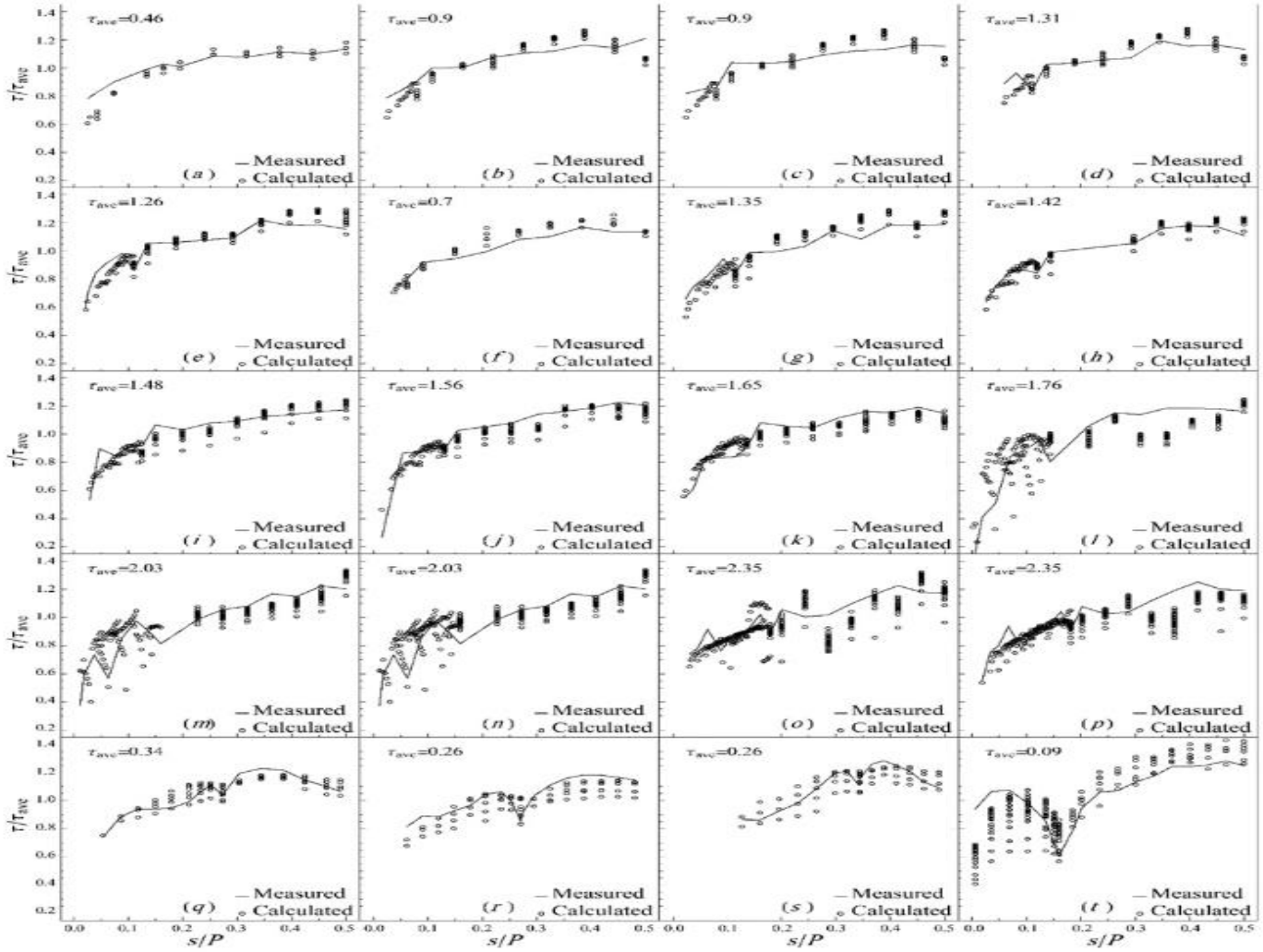

Fig.5. Normalized measured and calculated τ

Shear stress distribution along the wetted perimeter normalized by the mean value is shown in Fig. 5. The mean value of shear stress along the wetted perimeter for each case can also be seen in this Figure. According to ξ for local shear stress on the wetted perimeter, there are large discrepancies between the measured and calculated values in the cases with high MAPE. Similarly, this deviation is more apparent in the bed, especially near to centerline. In cases 040601_3 and 040802_3, the proposed model can not accurately estimate the shear stress for $0.3 < s/P < 0.45$, even for one of the points of recording velocity. In the case of S12, more values of estimated shear stress are smaller than the measured values for $s/P < 0.1$ and inversely are greater than measured data for $s/P > 0.15$. It is recommended to choose not very large amounts of d for recording velocity to get away from large errors.

4. Conclusion

The proposed Malvandi and Maghrebi (2021) model for estimating the shear stress distribution along the wetted perimeter is selected to verify only for trapezoidal cross sections. Although it has been calibrated and has good results for different sections containing two soft compound channels, it is necessary to calibrate it for some more compound channels before applying this model to rivers. As an objective function, the mean MAPE value between the model and the experimental data of some researchers is selected. To find the values of the model parameters, MAPE is minimized by a genetic algorithm.

In most cases, the error between the calculated and measured values of ξ is less than 10%. The average value of MAPE is 7.1%, although it varies from section to section. In two cases, the MAPE reaches a maximum value of about 16%, one of which is the rectangular cross-section with the sharpest angle in the boundary (90 degrees). In fifteen cases, the MAPE is less or about 7%. Measured and calculated by local shear stress model values are compared. Although the estimated values differ from the measured values in some points, especially at walls and corners, the model generally has good results. The most significant amounts of error between the calculated and measured values of both ξ and τ are found where the distance from the selected point for recording velocity to boundary d is considerable. It is more apparent in those parts of the wetted perimeter near the centerline. Therefore, to achieve better estimations of local shear stress on the boundary, recording velocity in the cross-section points not very far from the boundary, especially in the near parts of the bed to the centerline, is better.

Some or all data, models, or codes that support the findings of this study are available from the corresponding author upon reasonable request.

5 .References

1. Cheng, N.-S., 2007. Power-law index for velocity profiles in open channel flows. Advances in Water Resources 30(8), 1775-1784. https://doi.org/10.1016/j.advwatres.2007.02.001.
2. Dey, S., Lambert, F., 2005. Reynolds stress and bed shear in nonuniform unsteady open-channel flow. Journal of Hydraulic Engineering 131(7), 610-614. https://doi: 10.1061/(ASCE)0733-9429(2005)131:7(610).
3. Flintham, T. P., Carling, P. A., 1988. The prediction of mean bed and wall boundary shear in uniform and compositely rough channels. International conference on river regime, published by John Wiley & Sons Ltd. 267-287.
4. Ghosh, S. N., Roy, N., 1970. Boundary shear distribution in open channel flow. Journal of Hydraulics Division 96(4), 967-994. https://doi.org/10.1061/JYCEAJ.0002477.
5. Graham, D., James, P., Jones, T., Davies, J., Delo, E., 1992. Measurement and prediction of surface shear stress in annular flume. Journal of Hydraulic Engineering 118(9), 1270-1286. https://doi: 10.1061/(ASCE)0733-9429(1992)118:9(1270).
6. Khatua, K. K., Patra, K. C., 2007. Boundary shear stress distribution in compound open channel flow. ISH Journal of Hydraulic Engineering 13, 39-54. https://doi:10.1080/09715010.2007.10514882.
7. Khozani, Z.S., Bonakdari, H., Zaji, A.H., 2017. Using two soft computing methods to predict wall and bed shear stress in smooth rectangular channels. Appl Water Sci 7, 3973–3983. https://doi.org/10.1007/s13201-017-0548-y
8. Knight, D. W., 1981. Boundary shear in smooth and rough channels. Journal of Hydraulics Division 107(7), 839-851.
9. Knight, D. W., Demetriou, J. D., Hamed, M. E., 1984. Boundary shear in smooth rectangular channels. Journal of Hydraulic Engineering 110(4), 405-422.
10. Knight, D. W., Sellin, R. H. J., 1987. The SERC flood channel facility. Institution's River Engineering.
11. Knight, D. W., Shiono, K., 1990. Turbulence measurements in a shear layer region of a compound channel. Journal of Hydraulic Research 28(2), 175-196. https://doi:10.1080/00221689009499085.
12. Knight, D. W., Yuen, K. W. H., Alhamid, A. A. I., 1994. Boundary shear stress distributions in open channel flow, in Physical mechanisms of mixing and

transport in the environment. [Eds K. Beven, P. Chatwin & J. Millbank], J. Wiley, Chapter 4, 51-87.

13. Liepmann, H. W., Dhawan, S., 1952. Direct measurement of local skin friction in low speed and high speed flow. Proceedings, National Institute of Applied Mechanics, 869-874.

14. Malvandi, B., F. Maghrebi, M, 2021. Prediction of boundary shear stress distribution in straight open channels using velocity distribution. Water Science and Engineering. https://doi.org/10.1016/j.wse.2021.03.005.

15. Park, J. H., Kim, Y. D., Park, Y. S., Jo, J. A., Kang, K., 2016. Direct measurement of bottom shear stress under high-velocity flow conditions. Flow Measurement and Instrumentation. http://dx.doi.org/10.1016/j.flowmeasinst.2015.12.008.

16. Preston, J. H., 1954. The determination of turbulent skin friction by means of pitot tubes. Journal of Royal Aeronautical Society, London 58, 109-121. https://doi.org/10.1017/S0368393100097704.

17. Rankin, K. L., Hires, R. I., 2000. Laboratory measurement of bottom shear stress on a movable bed. Journal of Geophysical Research: Oceans 105(C7), 17011-17019. https://doi: 10.1029/2000JC900059.

18. Rhodes, D. G., Knight, D. W., 1994. Distribution of shear force on boundary of smooth rectangular duct. Journal of Hydraulic Engineering 120(7), 787-807. https://doi:10.1061/(ASCE)0733-9429(1994)120:7(787).

19. Tominaga, A., Nezu, I., Ezaki, K., Nakagawa, H., 1989. Three-dimensional turbulent structure in straight open channel flows. Journal of Hydraulic Research 27, 149-173. https://doi:10.1080/00221688909499249.

20. Wilcock, P. R., 1996. Estimating local bed shear stress from velocity observations. Water Resources Research 32(11), 3361-3366. https://doi: 10.1029/96WR02277.